

**Cumulative and individual impacts of the human
footprint on similarity to reference high ecological
integrity reference states.**

**Evan Muis¹, Nicholas Coops¹, Txomin Hermosilla², Chris Mulverhill¹, Cole
Burton¹, Stephen Ban³**

¹Department of Forest Resource Management, University of British Columbia, Vancouver, British
Columbia, Canada,

²Canadian Forest Service (Pacific Forestry Centre), Natural Resources Canada, Victoria, British
Columbia, Canada,

³BC Parks, Government of British Columbia, Victoria, British Columbia, Canada,

Corresponding author: Evan Muis, evanmuis@student.ubc.ca

Abstract

ABSTRACT

1 Introduction

A global biodiversity crisis is currently underway, driven by anthropogenic changes (Dirzo and Raven, 2003). Pressures such as climate change, land use change, and invasive species, are leading to species extinctions (Thomas et al., 2004; Urban, 2015) and the homogenization of biological communities (McGill et al., 2015). The Kunming-Montreal Global Biodiversity Framework (GBF) was adopted in December 2022 with the goal of restoring and safeguarding global biodiversity (Convention on Biological Diversity, 2023). Targets within this framework include restoring 30% of all degraded ecosystems, protecting 30% of the Earth’s terrestrial, inland water, and marine areas, and achieving no loss of high biodiversity importance areas, including high ecological integrity ecosystems (Convention on Biological Diversity, 2023). In the terrestrial environment, forest biomes have been shown to harbour the largest amount of biodiversity (Cardinale et al., 2012; Myers, 1988; Pimm and Raven, 2000), and provide key ecosystem services (Thompson et al., 2009). To provide these services, it is integral that these forest ecosystems are in good ecological condition, as represented by natural or near-natural levels of forest structure, function, and composition, often referred to as having high ecological integrity (Marín et al., 2021).

While understanding forest condition is a key aspect of understanding biodiversity and the provision of ecosystem services due to their inherent linkages (Cardinale et al., 2012; Marín et al., 2021), it is challenging to obtain suitable field-derived data across extensive land areas due to the significant financial and temporal costs associated with large-scale field campaigns. Remote sensing data, however, can provide a efficient and cost-effective alternative to field data, offering access to new spatially explicit and comprehensive datasets that can be linked to ecological condition, with additional metrics being proposed at a rapid pace (Pereira et al., 2013; Radeloff et al., 2024; Skidmore et al., 2021). Advances in lidar technologies and modelling methods are enabling the generation of wall-to-wall estimates of forest stand structure to be generated across entire countries (Becker et al., 2023; Matasci et al., 2018a; Matasci et al., 2018b), which serve as a more detailed indicator of ecosystem structure than the often previously used landscape fragmentation metrics (Andrew et al., 2012). Productivity metrics have been employed as a proxy for ecosystem function for many years (Pettorelli et al., 2018, 2005), with new Landsat-derived datasets providing integrative annual estimates of energy availability at a 30 m spatial resolution (Radeloff et al., 2024; Radeloff et al., 2019; Razenkova et al., n.d.). Remote sensing is quickly providing access to a vast array of datasets suitable for monitoring the various facets of biodiversity and ecological condition (Noss, 1990). The integration of these datasets with information pertaining to the location of known high-ecological-integrity forests enables researchers to identify high-quality forest reference states across entire jurisdictions, even in the presence of anthropogenic pressures.

Ecological reference states represent baseline conditions of ecosystems, serving as a benchmark for assessing ecological health and guiding restoration efforts (Nielsen et al., 2007). The application of counterfactual thinking, which entails considering the potential state of an ecosystem in the absence of anthropogenic pressures (Ferraro, 2009) can be instrumental for mapping high-integrity forests. Approaches such as coarsened exact matching (Iacus et al., 2012), can be used to facilitate comparisons between forest stands and their hypothetical reference states. These methods account for confounding environmental variables, thereby ensuring that all forests are compared to an appropriate reference state. Identifying a suitable reference state can be difficult, however there are methods which can be used to approximate high-integrity reference conditions. Historical reference states can be used when

an ecosystem has a large depth of temporal data to compare to, however, it is not always guaranteed that an ecosystem can be restored to these historical norms due to changing climates (Balaguer et al., 2014; McNellie et al., 2020). Other proposed methods for delineating baseline conditions include protected areas (Arcese and Sinclair, 1997), and empirical estimates of the reference state generated by modelling outcomes (oftentimes species abundances and occurrence) in the absence of anthropogenic disturbance (Nielsen et al., 2007).

Protected areas, specifically designed for biodiversity conservation, are frequently faced with lower levels anthropogenic pressure as a result of biases in their placement (Joppa and Pfaff, 2009; Muise et al., 2022). In forested ecosystems, over time this leads to undisturbed high-integrity forests remaining within protected areas due to their natural disturbance regimes and a lack of anthropogenic pressures (Brumelis et al., 2011). These high-integrity forests, situated within protected areas, can serve as effective ecological baselines (Arcese and Sinclair, 1997). When suitably matched to unprotected areas, they can be used as a reference state to assess the differences between all forests and their high-integrity counterparts (Ferraro, 2009). Further, protected areas and undisturbed ecosystems such as intact forest landscapes have been shown to have increased structural densities when compared to other ecosystems (Li et al., 2023; Muise et al., 2022).

Anthropogenic pressure such as increased road densities (Nielsen et al., 2007), harvesting leading to edge effects (Bourgoin et al., 2024), and other human-induced disturbances (Liira et al., 2007) have been shown to influence forest structure. Novel datasets such as the Forest Structural Condition Index (FSCA) have been developed which integrate both structure and anthropogenic pressure into an index which identifies ecosystems of high conservation value, with high structural complexity and low anthropogenic pressure (Hansen et al., 2019). The impacts of anthropogenic pressure on forest functioning and energy availability is less frequently assessed. Hedwall et al. (2019) assessed plant community shifts under anthropogenic pressures in the boreal forests of Sweden, and hypothesized that changed communities may affect forest functioning. Grantham et al. (2020) used forest extent and arrangement, alongside pressure datasets, to assess ecosystem integrity, with expectations that high-integrity ecosystems will retain high levels of ecosystem functioning. However, to our knowledge, direct impacts of anthropogenic pressures on forest ecosystem function have not been assessed at a landscape scale.

We proposed a novel, data-driven, approach to identify high-integrity forests based on various satellite-derived metrics of ecosystem condition, and calculate the degree of similarity for regions of unknown integrity to high-integrity forests found on Vancouver Island, British Columbia, Canada. We use a strict matching approach to ensure ecological similarity, and choose the highest 10% of metric values across variables that are known to be correlated with ecological condition and biodiversity. We then calculate ecological similarity using sigma dissimilarity (Mahony et al., 2017) alongside human footprint layers developed by Hirsh-Pearson et al. (2022) to assess the influence of anthropogenic pressure of ecological integrity by cumulative and individual pressures. Further, we compare the similarity metrics between ecological structure and function to identify linkages between ecological similarity of forest structure and forest functioning, while accounting for the presence of anthropogenic pressures.

2 Methods

2.1 Study Area

We focus on the forested areas of Vancouver Island, British Columbia, Canada. Vancouver island has approximately 31285 km² of land area, of which 79.5% is forested. The dominant forest species on Vancouver Island are Douglas-fir (*Pseudotsuga menziesii*), western red cedar (*Thuja plicata*), western hemlock (*Tsuga heterophylla*),

yellow cedar (*Chamaecyparis nootkatensis*), and Sitka spruce (*Picea sitchensis*) (Burns, 1990). British Columbia generally has a temperate maritime climate, with mild, wet winters, and cool, dry summers. There are four ecosystems on Vancouver Island as defined by British Columbia's biogeoclimatic ecosystem classification (BEC) framework (Pojar et al., 1987), Coastal Western Hemlock (CWH), Mountain Hemlock (MH), Coastal Douglas Fir (CDF), and Coastal Mountain-heather Alpine (CMA), which are broadly delineated based on soil, climate, and elevation. Forestry is an important industry on Vancouver Island, while fires are historically rare and low severity (Daniels and Gray, 2006).

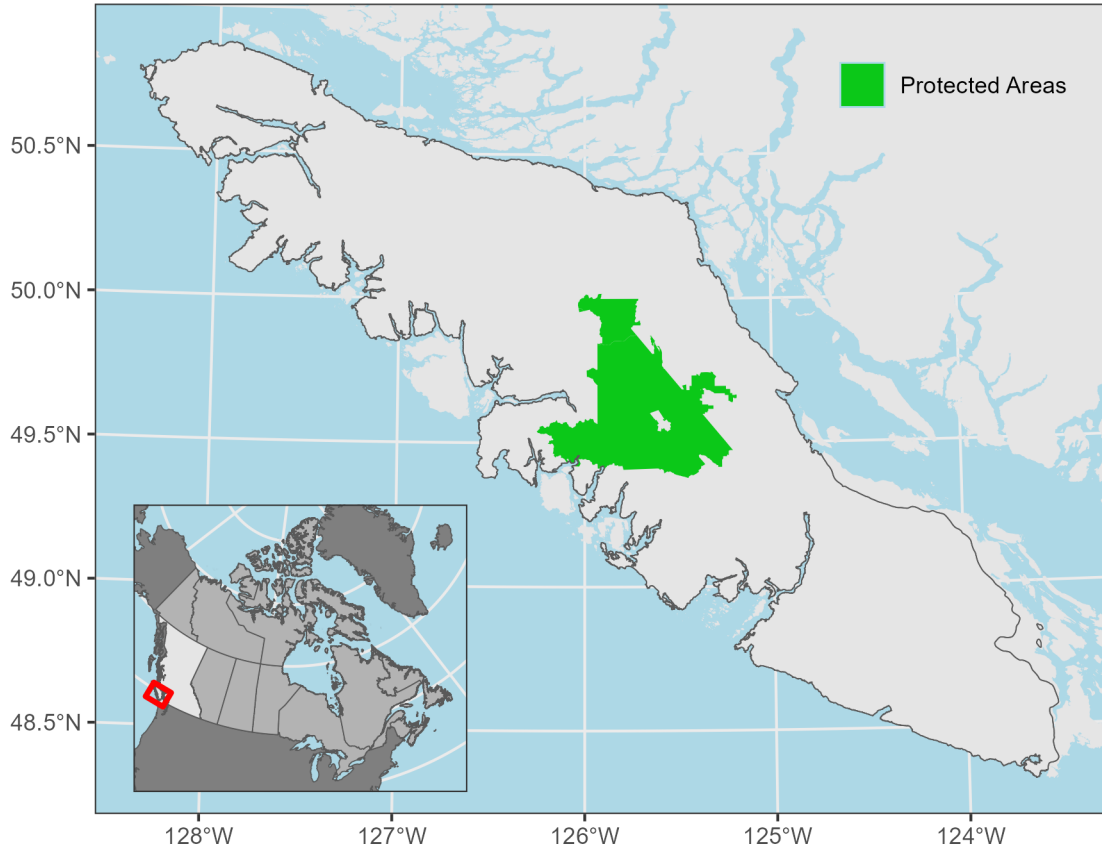


Figure 1: Study area on Vancouver Island, British Columbia, Canada, including the location of Strathcona Provincial Park.

2.2 Data

2.2.1 Reference State

We defined our reference state as the forested area of Strathcona Park. We chose Strathcona Park as a temporal and protected area reference state, as the oldest and largest (2480 km²) protected area in British Columbia. Strathcona Park was established in 1911, and 80% of the park is preserved as wilderness area and designated as Nature Conservancy Areas under the *Park Act* (“Park Act,” n.d.). The park contains three BEC zones, CWH, MH, and CMA, but does not include CDF, which is only found in the southern portion of the island. Due to this, we do not include CDF in our analysis.

2.2.2 Forest Structure

Wall-to-wall, 30 m forest structure metrics (canopy height, canopy cover, structural complexity, and aboveground biomass) were generated by Matasci et al. (2018a) for 2015 across the forested landscape of British Columbia. This data was generated by using a random forest-kNN approach, imputing airborne laser scanning derived forest structural attributes across the entirety of Canada using Landsat-derived best-available-pixel (BAP) composites (Hermosilla et al., 2016; White et al., 2014) and topographic information (Matasci et al., 2018a; Matasci et al., 2018b). The BAP composites were derived by selecting optical observations from the Landsat archive (including Landsat-5 Thematic Mapper, Landsat-7 Enhanced Thematic Mapper Plus, and Landsat-8 Operational Land Imager imagery) over the course of the growing season, considering atmospheric effects (haze, clouds, cloud shadows) and distance from the desired composite date (in this case, August 31st). Details on the pixel scoring method can be found in White et al. (2014). The BAP composites were further refined by using a spectral trend analysis on the normalized burn ratio to remove noise, and missing pixels are infilled using temporally-interpolated values. This procedure results in gap-free, surface-reflectance image composites (Hermosilla et al., 2015), which are used as the primary dataset to impute forest structural attributes (Matasci et al., 2018a; Matasci et al., 2018b).

2.2.3 Forest Function

For our forest ecosystem function dataset, we calculated the Dynamic Habitat Indices (Radeloff et al., 2019) using Landsat data on Google Earth Engine (Gorelick et al., 2017), following the methodology of Razenkova et al. (n.d.). Briefly, we created a synthetic year of NDVI composites using all available Landsat imagery from 2011-2020 (centred on 2015). We used the Landsat QA band derived from the fmask algorithm (Zhu and Woodcock, 2012) to filter out erroneous pixels, such as clouds and cloud shadows. Monthly NDVI values were calculated by taking the median of each month’s NDVI observations, ignoring the year the image was acquired. This allows us to generate the DHIs at spatial resolution of 30 m, while accounting for the lower temporal resolution of the Landsat series when compared to the more commonly used MODIS satellites (Razenkova et al., n.d.). The DHIs are calculated as the sum (Cumulative DHI), minimum (Minimum DHI), and coefficient of variation (Variation DHI) of these monthly observations. The three DHIs have been shown to be indicative of biodiversity over a range of scales (Radeloff et al., 2019; Razenkova et al., 2022) and extents (Coops et al., 2019, 2009) for a variety of clades (Michaud et al., 2014; Suttcliffe et al., 2021).

2.2.4 Anthropogenic Pressures

We use the Canadian Human Footprint as developed by Hirsh-Pearson et al. (2022). The Canadian Human Footprint is an additive pressure map generated by summing the 12 different anthropogenic pressures (built environments, crop land, pasture land, population density, nighttime lights, railways, roads, navigable waterways, dams and associated reservoirs, mining activity, oil and gas, and forestry), which ranges from zero to 55 for any cell across Canada. This cumulative dataset is also

distributed with Canada-wide individual pressure values (Hirsh-Pearson et al., n.d.). Here, we focus on the overall cumulative pressure map and four individual pressures: population density, built environments, roads, and forestry.

2.2.5 Covariates

In our matching procedure (see Section 2.3) we use two core datasets as our matching covariates. Firstly, we use a 30 m digital elevation model and derived slope dataset from the Advanced Spaceborne Thermal Emission and Reflection Radiometer (ASTER) Version 2 GDEM product (Tachikawa et al., 2011). We also match on four climate variables; mean annual precipitation (MAP), mean annual temperature (MAT), mean warmest month temperature (MWMT), and mean coldest month temperature (MCMT) calculated from 1990-2020 climate normals using the ClimateNA software package at a 1 km spatial resolution, and downsampled to 30 m using cubic spline resampling in the **terra** (version 1.7-71) R package (Hijmans, 2024) in R (R Core Team, 2024 version 4.4.1).

2.3 Calculating similarity

We calculate the sigma dissimilarity (Mahony et al., 2017) of forested pixels across British Columbia by using an expanded coarsened exact matching (CEM) technique, Figure 2. This methodology enables us to evaluate the degree of similarity between all forested pixels in the province and natural forests, while accounting for potential confounding variables such as climate and topography. Briefly, the CEM technique creates comparable groups of observations among covariates by initially coarsening the covariates. In this instance, all six covariates were coarsened into five quintiles hereafter referred to as bins. CEM then performs exact matching on the bins, with each pixel matched to a climatically and topographically similar group of pixels within Strathcona Park, hereafter referred to as strata. In the case where there is not enough matched pixels found in Strathcona Park, we calculate the nearest neighbours in bin space for all strata, and sample up to 1000 pixels while minimizing the nearest neighbour distance. If the nearest neighbour distance is on average above 2, we do not consider that strata in our analysis.

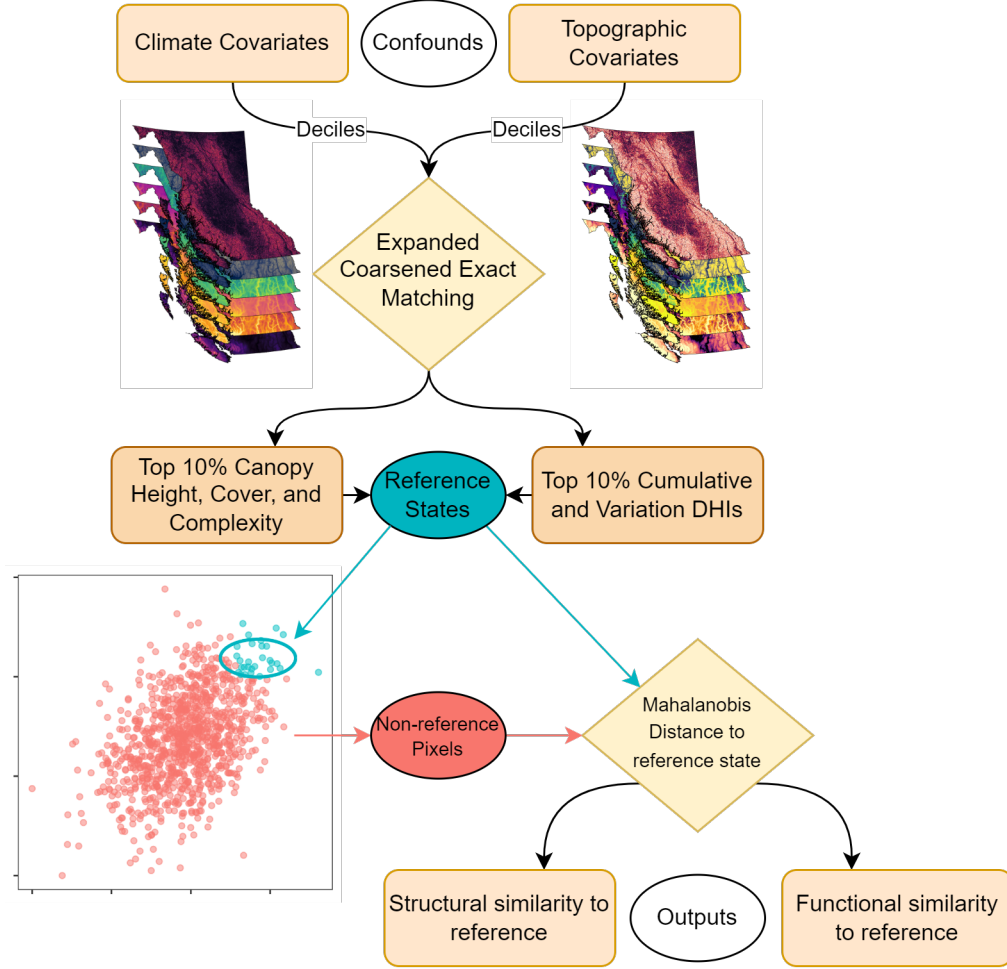


Figure 2: Conceptual flow diagram of the study.

Following the matching procedure, we identify data driven reference states in both structural and functional attributes by selecting the top 10% of protected observations for each structural (canopy height, cover, and structural complexity) and functional (cumulative and variation DHIs) attribute, separately. We then determine the similarity of all pixels, in both structural and functional attributes, to the reference states by calculating the sigma dissimilarity metric. Sigma dissimilarity standardizes the Mahalanobian distance (Mahalanobis, 1936) by rescaling it into percentiles of the chi distribution (Mahony et al., 2017). This effectively accounts for the effect of dimensionality when creating a multivariate similarity metric (Mahony et al., 2017). We calculate sigma dissimilarity for every strata with a suitable reference state, for each of the 6

2.4 Sampling

We reclassify the Canadian Human Footprint (Hirsh-Pearson et al., n.d.; Hirsh-Pearson et al., 2022) into categorical data following Hirsh-Pearson et al. (2022) and Arias-Patino et al. (2024) : a value of zero has no anthropogenic pressure, zero to four has low anthropogenic pressure, four to eight has medium anthropogenic pressure, and > eight has high anthropogenic pressure. To assess the cumulative impact of anthropogenic pressure on ecological similarity, we implement stratified sampling on all suitable strata, sampling 100 samples from each anthropogenic pressure

class. For our individual pressures, we follow the same reclassification steps on each pressure layer, and sample an additional hundred samples for each pressure class. Sampling was performed using the **sgsR** (version 1.4.5) R package (Goodbody et al., 2023) with the Quiennec method (Queinnec et al., 2021).

2.5 Analysis

We used a one-way analysis of variance (ANOVA) with a critical value of 0.05 to identify differences in the mean similarity values across cumulative anthropogenic pressure classes. We account for family-wise error rate for our ANOVAs using the Holm-Bonferroni method, only continuing the analysis for similarity variables with significant ANOVAs at the adjusted critical value. As ANOVAs only identify if there is a difference in means, but does not identify which means are different, we used a Tukey HSD post-hoc test to identify which means are different from the control group (no anthropogenic pressure), which also controls for the family-wise error rate.

We follow the same protocol to identify the difference in means for each anthropogenic pressure of interest (roads, population density, forestry, and built environment). We compare each pressure to the same ‘no pressure’ values sampled in the cumulative pressure analysis. All statistical analysis were conducted using the **rstatix** (version 0.7.2) R package (Kassambara, 2023).

3 Results

We found that similarity to high structural complexity (Anova: $p = 0.007$) and high canopy height (Anova: $p = 0.003$) reference states was influenced by medium to high levels of cumulative anthropogenic pressure (Figure 3). Similarity to high biomass (Anova: $p = 0.142$) and canopy cover (Anova: $p = 0.855$) regions were not significantly influenced by cumulative anthropogenic pressures. Productivity metrics were also not influenced by cumulative anthropogenic pressures.

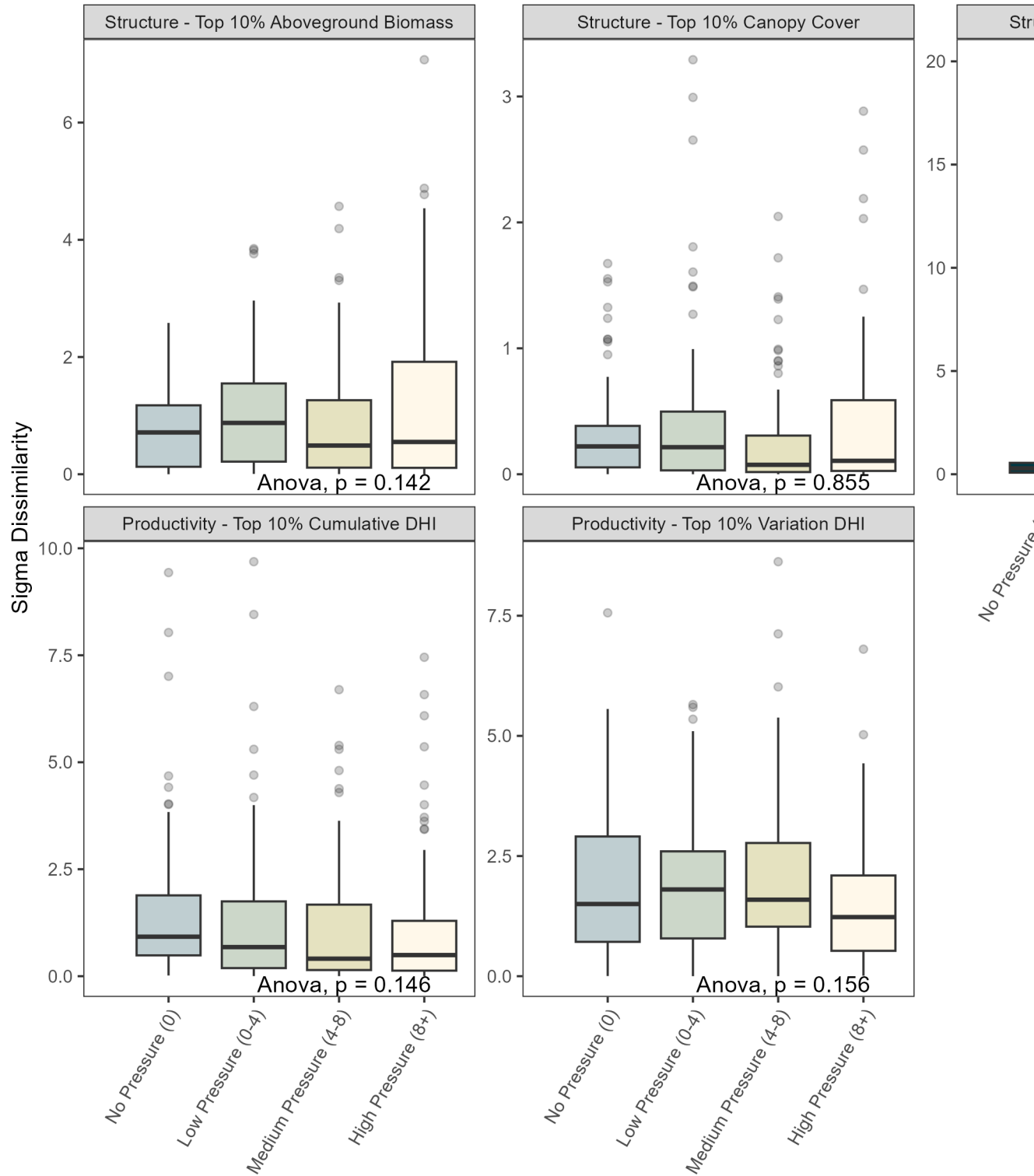


Figure 3: Boxplots of sigma similarity to the reference state in Strathcona Provincial Park by cumulative human footprint category. Anova p-values corrected using the Holm-Bonferroni method. * indicates a Tukey HSD p-value < 0.05. ** indicates a Tukey HSD p-value < 0.01.

Increases in all individual anthropogenic pressures led to increased dissimilarity when compared to most structural reference states (Figure 4). Increases in pressures from roads and built environment did not increase or reduce similarity to structural reference states with high canopy cover. Medium and high pressures from population density and forestry/harvesting increased dissimilarity to all structural reference states. Anthropogenic pressures generally did not influence the similarity to reference states based on productivity metrics, however, increases in pressures from population density decreased dissimilarity to ecosystems with high variation in energy availability.

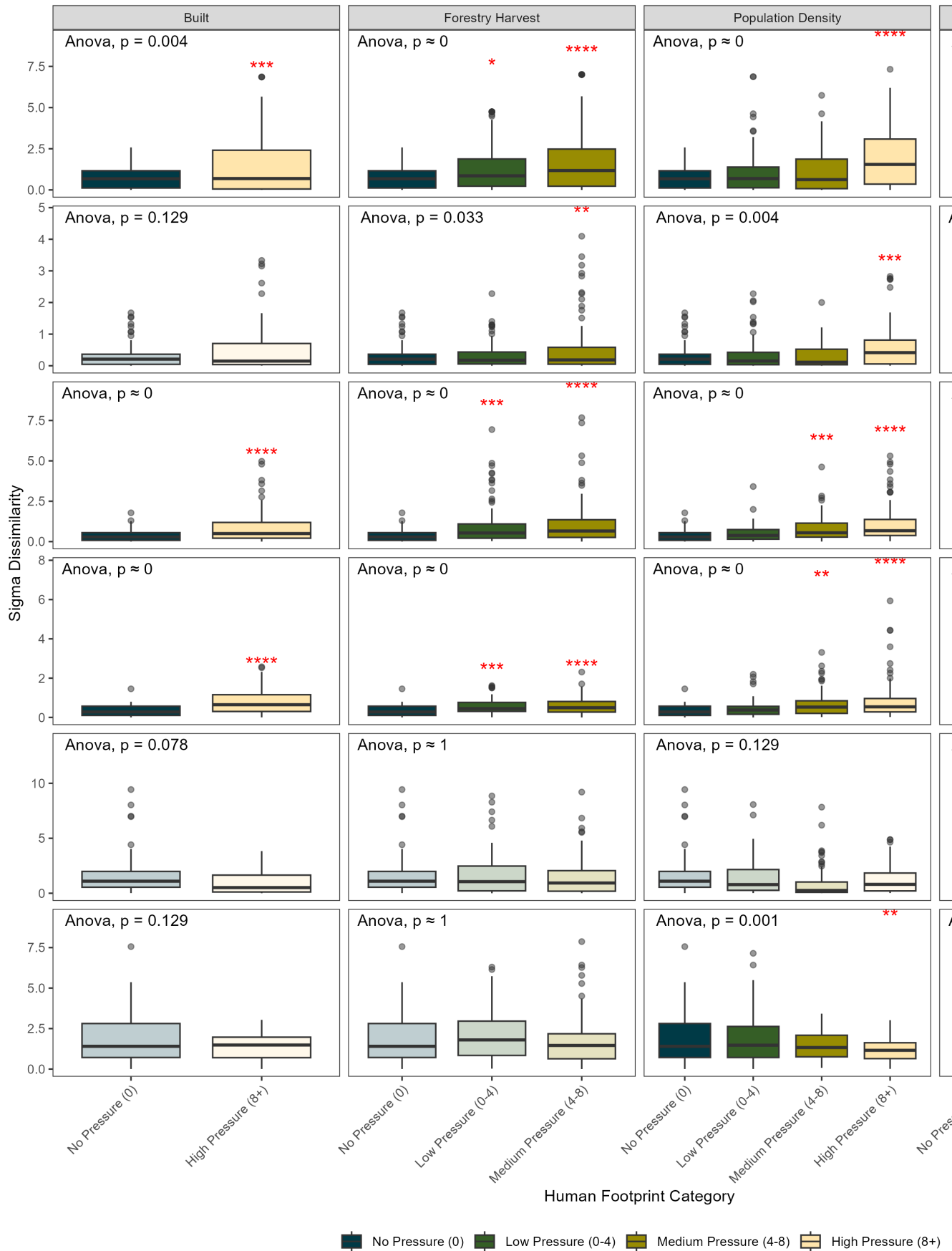


Figure 4: Boxplots of sigma similarity to the reference state in Strathcona Provincial Park by individual anthropogenic pressures. Anova p-values corrected using the Holm-Bonferroni method. * indicates a Tukey HSD p-value < 0.05. ** indicates a Tukey HSD p-value < 0.01. *** indicates a Tukey HSD p-value < 0.001. **** indicates a Tukey HSD p-value < 0.0001.

4 Discussion

In this paper, we use medium-resolution remote sensing metrics of ecosystem structure and function to assess similarity to high-integrity forests across Vancouver Island, British Columbia. We validate our approach by assessing the influence of the human footprint on these reference states, finding that ecosystem structure in the form of forest structural attributes is influenced by increased anthropogenic pressures on a cumulative and individual level (Figure 3; Figure 4). Forest ecosystem function, as represented by the DHIs, is generally not significantly influenced by anthropogenic pressures, although population density increased similarity to ecosystems with high variation in energy availability (Figure 4).

We find that similarity to high structural complexity forests, which are often high in biodiversity due to increased niche availability (Macarthur and Macarthur, 1961; Walter et al., 2021), is impacted by medium to high levels of anthropogenic pressures. Structural similarity to tall forests is also impacted by medium to high levels of anthropogenic pressure, while productivity metrics were not influenced by cumulative anthropogenic pressures in this region (Figure 3). In tropical forests, Bourgoïn et al. (2024) found that anthropogenic forest degradation influenced aboveground biomass and canopy height, however, they focus on edge effects, fire, and selective logging, rather than cumulative and individual anthropogenic pressures. Li et al. (2023) also found a global impact of anthropogenic pressures on forest structural density, however, they do not explore which facets of anthropogenic pressure are the strongest driver of forest degradation. Hansen et al. (2020) integrate forest structure and anthropogenic pressure into the forest structural integrity index to identify forest stands of high ecological value (high structural quality; low anthropogenic footprint). We further this research by assessing individual pressures on a multivariate metric of structural similarity to a high-quality reference state (Figure 4).

Anthropogenic effects on forest function are rarely examined. Here, we also examine how anthropogenic pressures influence similarity to high available energy and high energy variation forests, both hypothesized to indicate high levels of biodiversity in a number of guilds and clades (Radeloff et al., 2019; Razenkova et al., 2022). We do not find a strong influence of cumulative anthropogenic pressure on our forest functioning metrics, however, we did find that dissimilarity to forest stands with high annual energy variability was reduced under high anthropogenic pressure (Figure 4).

Assessing individual pressure influences on the environment is also relevant to questions of how cumulative anthropogenic pressure maps are calculate. There is currently a debate between additive and antagonistic anthropogenic pressure mapping methods, as there is little information on mechanistic interactions between pressures (Arias-Patino et al., 2024). We assess individual pressures on structural and functional similarity in forests across Vancouver Island, Canada, an advancement upon the current standard of using a single value of cumulative anthropogenic pressure (Bourgoïn et al., 2024; Li et al., 2023). Similar methods could be used to examine mechanistic pressure interactions across large scales.

We apply the Sigma Dissimilarity metric developed by Mahony et al. (2017) to determine similarity to high-integrity ecosystems, and use a matching approach to account for environmental covariates. This method accounts for the multidimensionality of the structure and function datasets, and standardizes them so they are comparable. This is especially relevant in our case as we use four forest structural attributes and two forest function metrics. These methods are similar to other similarity metrics commonly applied in remote sensing for multivariate similarity such as spectral similarity (Schweiger et al., 2018), and phenospectral similarity (Osei Darko et al., 2024).

While we are limited in number of structural variables due to the imputation of the lidar-derived dataset across the study area (Matasci et al., 2018a; Matasci et al.,

2018b), future studies could directly use raw lidar datasets to create a multitude of metrics, and apply the sigma similarity method to those. This could capture additional facets of similarity which are missed when using a Canada-wide dataset with limited forest structural attributes at 30 m. New spaceborne lidar missions such as GEDI (Dubayah et al., 2020) and IceSAT-II (Neumann et al., 2019) are also providing estimates of forest structure across the globe. However, these satellites are sample based missions, and do not provide wall-to-wall coverage (Duncanson et al., 2021).

We assess multiple definitions of high quality forest across a large region using a data-driven approach. Often, it is common for reference states to be unavailable due to a lack of data on regions of high ecological integrity, especially across large regions (McNellie et al., 2020). We attempt to circumvent this by using a large, long-established protected area (Strathcona Provincial Park; Figure 1), and a matching technique that preserves ecological similarity between reference states and their counterparts. The long-established, large protected area ensures that little anthropogenic pressures or modification have been made to the landscape, while also guaranteeing that the reference state is attainable for a given topography and climate (Corlett, 2016; Hobbs et al., 2014) due to contemporary nature of the reference state. Our matching technique (coarsened exact matching, combined with an kNN approach when no exact match is available) allows us to generate reference states in a near wall-to-wall fashion, which ensures similarity between reference state and compared pixels.

Our techniques move beyond traditional impact evaluation techniques (Ferraro, 2009) commonly used in protected area effectiveness assessments by allowing spatial reconstruction of conservation outcomes, and generating a multivariate, rather than univariate, assessment of similarity to high ecological integrity forests. While our methods in this paper use a data-driven approach to derive reference states, if an individual or organization is interested in a specific species or ecosystem, and has known locations of high quality ecosystems associated with that species or ecosystem, these methods can be applied to assess similarity to those high quality ecosystems across large regions.

Could also be a paragraph about urban forestry and canopy cover. Since urban foresters want to preserve high amounts of cover and greenspace that could be why the roads/built environments don't see strong differences to the reference state. This issue is also compounded by the canopy cover on the island just being consistently high across the board. I'm fine not discussing this, but could be something interesting to note

References

- Andrew, M.E., Wulder, M.A., Coops, N.C., 2012. Identification of *de facto* protected areas in boreal Canada. *Biological Conservation* 146, 97–107. <https://doi.org/10.1016/j.biocon.2011.11.029>
- Arcese, P., Sinclair, A.R.E., 1997. The role of protected areas as ecological baselines. *The Journal of Wildlife Management* 61, 587–602. <https://doi.org/10.2307/3802167>
- Arias-Patino, M., Johnson, C.J., Schuster, R., Wheate, R.D., Venter, O., 2024. Accuracy, uncertainty, and biases in cumulative pressure mapping. *Ecological Indicators* 166, 112407. <https://doi.org/10.1016/j.ecolind.2024.112407>
- Balaguer, L., Escudero, A., Martín-Duque, J.F., Mola, I., Aronson, J., 2014. The historical reference in restoration ecology: Re-defining a cornerstone concept. *Biological Conservation* 176, 12–20. <https://doi.org/10.1016/j.biocon.2014.05.007>

- Becker, A., Russo, S., Puliti, S., Lang, N., Schindler, K., Wegner, J.D., 2023. Country-wide retrieval of forest structure from optical and SAR satellite imagery with deep ensembles. *ISPRS Journal of Photogrammetry and Remote Sensing* 195, 269–286. <https://doi.org/10.1016/j.isprsjprs.2022.11.011>
- Bourgoin, C., Ceccherini, G., Girardello, M., Vancutsem, C., Avitabile, V., Beck, P.S.A., Beuchle, R., Blanc, L., Duveiller, G., Migliavacca, M., Vieilledent, G., Cescatti, A., Achard, F., 2024. Human degradation of tropical moist forests is greater than previously estimated. *Nature* 631, 570–576. <https://doi.org/10.1038/s41586-024-07629-0>
- Brumelis, G., Jonsson, B.G., Kouki, J., Kuuluvainen, T., Shorohova, E., 2011. *Forest naturalness in northern Europe: perspectives on processes, structures and species diversity*. *Silva Fennica* 45.
- Burns, R.M., 1990. *Silvics of North America*. U.S. Department of Agriculture, Forest Service.
- Cardinale, B.J., Duffy, J.E., Gonzalez, A., Hooper, D.U., Perrings, C., Venail, P., Narwani, A., Mace, G.M., Tilman, D., Wardle, D.A., Kinzig, A.P., Daily, G.C., Loreau, M., Grace, J.B., Larigauderie, A., Srivastava, D.S., Naeem, S., 2012. Biodiversity loss and its impact on humanity. *Nature* 486, 59–67. <https://doi.org/10.1038/nature11148>
- Convention on Biological Diversity, 2023. Report of the conference of the parties to the Convention on Biological Diversity on the second part of its fifteenth meeting (No. CBD/COP/15/17).
- Coops, N.C., Bolton, D.K., Hobi, M.L., Radeloff, V.C., 2019. Untangling multiple species richness hypothesis globally using remote sensing habitat indices. *Ecological Indicators* 107. <https://doi.org/10.1016/j.ecolind.2019.105567>
- Coops, N.C., Waring, R.H., Wulder, M.A., Pidgeon, A.M., Radeloff, V.C., 2009. Bird diversity: A predictable function of satellite-derived estimates of seasonal variation in canopy light absorbance across the united states. *JOURNAL OF BIOGEOGRAPHY* 36, 905–918. <https://doi.org/10.1111/j.1365-2699.2008.02053.x>
- Corlett, R.T., 2016. Restoration, reintroduction, and rewilding in a changing world. *Trends in Ecology & Evolution* 31, 453–462. <https://doi.org/10.1016/j.tree.2016.02.017>
- Daniels, L.D., Gray, R.W., 2006. Disturbance regimes in coastal British Columbia. *Journal of Ecosystems and Management* 7. <https://doi.org/10.22230/jem.2006v7n2a542>
- Dirzo, R., Raven, P.H., 2003. Global State of Biodiversity and Loss. *Annual Review of Environment and Resources* 28, 137–167. <https://doi.org/10.1146/annurev.energy.28.050302.105532>
- Dubayah, R., Blair, J.B., Goetz, S., Fatoyinbo, L., Hansen, M., Healey, S., Hofton, M., Hurtt, G., Kellner, J., Luthcke, S., Armston, J., Tang, H., Duncanson, L., Hancock, S., Jantz, P., Marselis, S., Patterson, P.L., Qi, W., Silva, C., 2020. The Global Ecosystem Dynamics Investigation: High-resolution laser ranging of the Earth's forests and topography. *Science of Remote Sensing* 1, 100002. <https://doi.org/10.1016/j.srs.2020.100002>
- Duncanson, L., Neuenschwander, A., Silva, C.A., Montesano, P., Guenther, E., Thomas, N., Hancock, S., Minor, D., White, J., Wulder, M., Armston, J., 2021. 2021 IEEE international geoscience and remote sensing symposium IGARSS. pp. 670–672. <https://doi.org/10.1109/IGARSS47720.2021.9553209>
- Ferraro, P.J., 2009. Counterfactual thinking and impact evaluation in environmental policy. *New Directions for Evaluation* 2009, 75–84. <https://doi.org/10.1002/ev.297>
- Goodbody, T.R.H., Coops, N.C., Queinnec, M., White, J.C., Tompalski, P., Hudak, A.T., Auty, D., Valbuena, R., LeBoeuf, A., Sinclair, I., McCartney, G., Prieur, J.-F., Woods, M.E., 2023. sgsR: A structurally guided sampling toolbox for

- LiDAR-based forest inventories. *Forestry: An International Journal of Forest Research* cpac055. <https://doi.org/10.1093/forestry/cpac055>
- Gorelick, N., Hancher, M., Dixon, M., Ilyushchenko, S., Thau, D., Moore, R., 2017. Google Earth Engine: Planetary-scale geospatial analysis for everyone. *Remote Sensing of Environment, Big Remotely Sensed Data: tools, applications and experiences* 202, 18–27. <https://doi.org/10.1016/j.rse.2017.06.031>
- Grantham, H.S., Duncan, A., Evans, T.D., Jones, K.R., Beyer, H.L., Schuster, R., Walston, J., Ray, J.C., Robinson, J.G., Callow, M., Clements, T., Costa, H.M., DeGemmis, A., Elsen, P.R., Ervin, J., Franco, P., Goldman, E., Goetz, S., Hansen, A., Hofsvang, E., Jantz, P., Jupiter, S., Kang, A., Langhammer, P., Laurance, W.F., Lieberman, S., Linkie, M., Malhi, Y., Maxwell, S., Mendez, M., Mittermeier, R., Murray, N.J., Possingham, H., Radachowsky, J., Saatchi, S., Samper, C., Silverman, J., Shapiro, A., Strassburg, B., Stevens, T., Stokes, E., Taylor, R., Tear, T., Tizard, R., Venter, O., Visconti, P., Wang, S., Watson, J.E.M., 2020. Anthropogenic modification of forests means only 40. *Nature Communications* 11, 5978. <https://doi.org/10.1038/s41467-020-19493-3>
- Hansen, A., Barnett, K., Jantz, P., Phillips, L., Goetz, S.J., Hansen, M., Venter, O., Watson, J.E.M., Burns, P., Atkinson, S., Rodríguez-Buritica, S., Ervin, J., Virnig, A., Supples, C., De Camargo, R., 2019. Global humid tropics forest structural condition and forest structural integrity maps. *Scientific Data* 6, 232. <https://doi.org/10.1038/s41597-019-0214-3>
- Hansen, A.J., Burns, P., Ervin, J., Goetz, S.J., Hansen, M., Venter, O., Watson, J.E.M., Jantz, P.A., Virnig, A.L.S., Barnett, K., Pillay, R., Atkinson, S., Supples, C., Rodríguez-Buritica, S., Armenteras, D., 2020. A policy-driven framework for conserving the best of Earth’s remaining moist tropical forests. *Nature Ecology & Evolution* 4, 1377–1384. <https://doi.org/10.1038/s41559-020-1274-7>
- Hedwall, P.-O., Gustafsson, L., Brunet, J., Lindblad, M., Axelsson, A.-L., Strebom, J., 2019. Half a century of multiple anthropogenic stressors has altered northern forest understory plant communities. *ECOLOGICAL APPLICATIONS* 29, e01874. <https://doi.org/10.1002/eap.1874>
- Hermosilla, T., Wulder, M.A., White, J.C., Coops, N.C., Hobart, G.W., 2015. An integrated landsat time series protocol for change detection and generation of annual gap-free surface reflectance composites. *Remote Sensing of Environment* 158, 220234. <https://doi.org/10.1016/j.rse.2014.11.005>
- Hermosilla, T., Wulder, M.A., White, J.C., Coops, N.C., Hobart, G.W., Campbell, L.B., 2016. Mass data processing of time series landsat imagery: Pixels to data products for forest monitoring. *International Journal of Digital Earth* 9, 10351054. <https://doi.org/10.1080/17538947.2016.1187673>
- Hijmans, R.J., 2024. *Terra: Spatial data analysis*.
- Hirsh-Pearson, K., Johnson, C.J., Schuster, R., Wheate, R.D., Venter, O., 2022. Canada’s human footprint reveals large intact areas juxtaposed against areas under immense anthropogenic pressure. *FACETS* 7, 398–419. <https://doi.org/10.1139/facets-2021-0063>
- Hirsh-Pearson, K., Johnson, C., Schuster, R., Wheate, R., Venter, O., n.d. The Canadian Human Footprint. <https://doi.org/10.5683/SP2/EVKA VL>
- Hobbs, R.J., Higgs, E., Hall, C.M., Bridgewater, P., Chapin III, F.S., Ellis, E.C., Ewel, J.J., Hallett, L.M., Harris, J., Hulvey, K.B., Jackson, S.T., Kennedy, P.L., Kueffer, C., Lach, L., Lantz, T.C., Lugo, A.E., Mascaro, J., Murphy, S.D., Nelson, C.R., Perring, M.P., Richardson, D.M., Seastedt, T.R., Standish, R.J., Starzomski, B.M., Suding, K.N., Tognetti, P.M., Yakob, L., Yung, L., 2014. Managing the whole landscape: historical, hybrid, and novel ecosystems. *Frontiers in Ecology and the Environment* 12, 557–564. <https://doi.org/10.1890/130300>
- Iacus, S.M., King, G., Porro, G., 2012. Causal Inference without Balance Checking: Coarsened Exact Matching. *Political Analysis* 20, 1–24. <https://doi.org/10.1093/pan/mpr013>

- Joppa, L.N., Pfaff, A., 2009. High and Far: Biases in the Location of Protected Areas. *PLOS ONE* 4, e8273. <https://doi.org/10.1371/journal.pone.0008273>
- Kassambara, A., 2023. *Rstatix: Pipe-friendly framework for basic statistical tests*.
- Li, W., Guo, W.-Y., Pasgaard, M., Niu, Z., Wang, L., Chen, F., Qin, Y., Svenning, J.-C., 2023. Human fingerprint on structural density of forests globally. *Nature Sustainability* 6, 368–379. <https://doi.org/10.1038/s41893-022-01020-5>
- Liira, J., Sepp, T., Parrest, O., 2007. The forest structure and ecosystem quality in conditions of anthropogenic disturbance along productivity gradient. *Forest Ecology and Management, Disturbances at multiple scales as the basis of forest ecosystem restoration and management* 250, 34–46. <https://doi.org/10.1016/j.foreco.2007.03.007>
- Macarthur, R., Macarthur, J., 1961. On bird species-diversity. *Ecology* 42, 594– &. <https://doi.org/10.2307/1932254>
- Mahalanobis, P.C., 1936. On the generalized distance in statistics. *Proceedings of the National Institute of Sciences (Calcutta)* 2, 4955.
- Mahony, C.R., Cannon, A.J., Wang, T., Aitken, S.N., 2017. A closer look at novel climates: new methods and insights at continental to landscape scales. *Global Change Biology* 23, 3934–3955. <https://doi.org/10.1111/gcb.13645>
- Marín, A.I., Abdul Malak, D., Bastrup-Birk, A., Chirici, G., Barbati, A., Kleeschulte, S., 2021. Mapping forest condition in europe: Methodological developments in support to forest biodiversity assessments. *Ecological Indicators* 128, 107839. <https://doi.org/10.1016/j.ecolind.2021.107839>
- Matasci, G., Hermosilla, T., Wulder, M.A., White, J.C., Coops, N.C., Hobart, G.W., Bolton, D.K., Tompalski, P., Bater, C.W., 2018a. Three decades of forest structural dynamics over canada’s forested ecosystems using landsat time-series and lidar plots. *Remote Sensing of Environment* 216, 697714. <https://doi.org/10.1016/j.rse.2018.07.024>
- Matasci, G., Hermosilla, T., Wulder, M.A., White, J.C., Coops, N.C., Hobart, G.W., Zald, H.S.J., 2018b. Large-area mapping of Canadian boreal forest cover, height, biomass and other structural attributes using Landsat composites and lidar plots. *Remote Sensing of Environment* 209, 90–106. <https://doi.org/10.1016/j.rse.2017.12.020>
- McGill, B.J., Dornelas, M., Gotelli, N.J., Magurran, A.E., 2015. Fifteen forms of biodiversity trend in the Anthropocene. *Trends in Ecology & Evolution* 30, 104–113. <https://doi.org/10.1016/j.tree.2014.11.006>
- McNellie, M.J., Oliver, I., Dorrough, J., Ferrier, S., Newell, G., Gibbons, P., 2020. Reference state and benchmark concepts for better biodiversity conservation in contemporary ecosystems. *Global Change Biology* 26, 6702–6714. <https://doi.org/10.1111/gcb.15383>
- Michaud, J.-S., Coops, N.C., Andrew, M.E., Wulder, M.A., Brown, G.S., Rickbeil, G.J.M., 2014. Estimating moose (alces alces) occurrence and abundance from remotely derived environmental indicators. *REMOTE SENSING OF ENVIRONMENT* 152, 190–201. <https://doi.org/10.1016/j.rse.2014.06.005>
- Muise, E.R., Coops, N.C., Hermosilla, T., Ban, S.S., 2022. Assessing representation of remote sensing derived forest structure and land cover across a network of protected areas. *Ecological Applications* 32, e2603. <https://doi.org/10.1002/eap.2603>
- Myers, N., 1988. Threatened biotas: "Hot spots" in tropical forests. *Environmentalist* 8, 187–208. <https://doi.org/10.1007/BF02240252>
- Neumann, T.A., Martino, A.J., Markus, T., Bae, S., Bock, M.R., Brenner, A.C., Brunt, K.M., Cavanaugh, J., Fernandes, S.T., Hancock, D.W., Harbeck, K., Lee, J., Kurtz, N.T., Luers, P.J., Luthcke, S.B., Magruder, L., Pennington, T.A., Ramos-Izquierdo, L., Rebold, T., Skoog, J., Thomas, T.C., 2019. The Ice, Cloud, and Land Elevation Satellite – 2 mission: A global geolocated photon product de-

- rived from the Advanced Topographic Laser Altimeter System. *Remote Sensing of Environment* 233, 111325. <https://doi.org/10.1016/j.rse.2019.111325>
- Nielsen, S.E., Bayne, E.M., Schieck, J., Herbers, J., Boutin, S., 2007. A new method to estimate species and biodiversity intactness using empirically derived reference conditions. *Biological Conservation* 137, 403–414. <https://doi.org/10.1016/j.biocon.2007.02.024>
- Noss, R.F., 1990. Indicators for Monitoring Biodiversity: A Hierarchical Approach. *Conservation Biology* 4, 355–364. <https://doi.org/10.1111/j.1523-1739.1990.tb00309.x>
- Osei Darko, P., Laliberté, E., Kalacska, M., Arroyo-Mora, J.P., Gonzalez, A., Zuloaga, J., 2024. Phenospectral similarity as an index of ecological integrity. *Frontiers in Environmental Science* 12. <https://doi.org/10.3389/fenvs.2024.1333762>
- Park Act*, n.d. RSBC 1996, c 344.
- Pereira, H.M., Ferrier, S., Walters, M., Geller, G.N., Jongman, R.H.G., Scholes, R.J., Bruford, M.W., Brummitt, N., Butchart, S.H.M., Cardoso, A.C., Coops, N.C., Dulloo, E., Faith, D.P., Freyhof, J., Gregory, R.D., Heip, C., Hoft, R., Hurtt, G., Jetz, W., Karp, D.S., McGeoch, M.A., Obura, D., Onoda, Y., Pettorelli, N., Reyers, B., Sayre, R., Scharlemann, J.P.W., Stuart, S.N., Turak, E., Walpole, M., Wegmann, M., 2013. Essential Biodiversity Variables. *Science* 339, 277–278. <https://doi.org/10.1126/science.1229931>
- Pettorelli, N., Schulte to Bühne, H., Tulloch, A., Dubois, G., Macinnis-Ng, C., Queirós, A.M., Keith, D.A., Wegmann, M., Schrod, F., Stellmes, M., Sonnenschein, R., Geller, G.N., Roy, S., Somers, B., Murray, N., Bland, L., Geijendorffer, I., Kerr, J.T., Broszeit, S., Leitão, P.J., Duncan, C., El Serafy, G., He, K.S., Blanchard, J.L., Lucas, R., Mairota, P., Webb, T.J., Nicholson, E., 2018. Satellite remote sensing of ecosystem functions: opportunities, challenges and way forward. *Remote Sensing in Ecology and Conservation* 4, 71–93. <https://doi.org/10.1002/rse2.59>
- Pettorelli, N., Vik, J.O., Mysterud, A., Gaillard, J.-M., Tucker, C.J., Stenseth, N.Chr., 2005. Using the satellite-derived NDVI to assess ecological responses to environmental change. *Trends in Ecology & Evolution* 20, 503–510. <https://doi.org/10.1016/j.tree.2005.05.011>
- Pimm, S.L., Raven, P., 2000. Extinction by numbers. *Nature* 403, 843–845. <https://doi.org/10.1038/35002708>
- Pojar, J., Klinka, K., Meidinger, D.V., 1987. Biogeoclimatic ecosystem classification in British Columbia. *Forest Ecology and Management* 22, 119–154. [https://doi.org/10.1016/0378-1127\(87\)90100-9](https://doi.org/10.1016/0378-1127(87)90100-9)
- Queinnec, M., White, J.C., Coops, N.C., 2021. Comparing airborne and spaceborne photon-counting LiDAR canopy structural estimates across different boreal forest types. *Remote Sensing of Environment* 262, 112510. <https://doi.org/10.1016/j.rse.2021.112510>
- R Core Team, 2024. *R: A language and environment for statistical computing*. R Foundation for Statistical Computing, Vienna, Austria.
- Radeloff, V.C., Dubinin, M., Coops, N.C., Allen, A.M., Brooks, T.M., Clayton, M.K., Costa, G.C., Graham, C.H., Helmers, D.P., Ives, A.R., Kolesov, D., Pidgeon, A.M., Rapacciuolo, G., Razenkova, E., Suttidate, N., Young, B.E., Zhu, L., Hobi, M.L., 2019. The Dynamic Habitat Indices (DHIs) from MODIS and global biodiversity. *Remote Sensing of Environment* 222, 204–214. <https://doi.org/10.1016/j.rse.2018.12.009>
- Radeloff, V.C., Roy, D.P., Wulder, M.A., Anderson, M., Cook, B., Crawford, C.J., Friedl, M., Gao, F., Gorelick, N., Hansen, M., Healey, S., Hostert, P., Hulley, G., Huntington, J.L., Johnson, D.M., Neigh, C., Lyapustin, A., Lymburner, L., Pahlevan, N., Pekel, J.-F., Scambos, T.A., Schaaf, C., Strobl, P., Woodcock, C.E., Zhang, H.K., Zhu, Z., 2024. Need and vision for global medium-resolution

- landsat and sentinel-2 data products. *Remote Sensing of Environment* 300, 113918. <https://doi.org/10.1016/j.rse.2023.113918>
- Razenkova, E., Farwell, L.S., Elsen, P., Carroll, K.A., Pidgeon, A.M., Radeloff, V., 2022. Explaining bird richness with the dynamic habitat indices across the conterminous US 2022, B15A–05.
- Razenkova, E., Lewińska, K.E., Yin, H., Farwell, L.S., Pidgeon, A.M., Hostert, P., Coops, N.C., Radeloff, V.C., n.d. Medium-resolution dynamic habitat indices from landsat satellite imagery. *Remote Sensing of Environment*.
- Schweiger, A.K., Cavender-Bares, J., Townsend, P.A., Hobbie, S.E., Madritch, M.D., Wang, R., Tilman, D., Gamon, J.A., 2018. Plant spectral diversity integrates functional and phylogenetic components of biodiversity and predicts ecosystem function. *Nature Ecology & Evolution* 2, 976–982. <https://doi.org/10.1038/s41559-018-0551-1>
- Skidmore, A.K., Coops, N.C., Neinavaz, E., Ali, A., Schaepman, M.E., Paganini, M., Kissling, W.D., Vihervaara, P., Darvishzadeh, R., Feilhauer, H., Fernandez, M., Fernández, N., Gorelick, N., Geijzenborffer, I., Heiden, U., Heurich, M., Hobern, D., Holzwarth, S., Muller-Karger, F.E., Van De Kerchove, R., Lausch, A., Leitão, P.J., Lock, M.C., Múcher, C.A., O'Connor, B., Rocchini, D., Turner, W., Vis, J.K., Wang, T., Wegmann, M., Wingate, V., 2021. Priority list of biodiversity metrics to observe from space. *Nature Ecology & Evolution*. <https://doi.org/10.1038/s41559-021-01451-x>
- Suttidate, N., Steinmetz, R., Lynam, A.J., Sukmasuang, R., Ngoprasert, D., Chutipong, W., Bateman, B.L., Jenks, K.E., Baker-Whatton, M., Kitamura, S., Ziolkowska, E., Radeloff, V.C., 2021. Habitat connectivity for endangered indochinese tigers in thailand. *GLOBAL ECOLOGY AND CONSERVATION* 29. <https://doi.org/10.1016/j.gecco.2021.e01718>
- Tachikawa, T., Kaku, M., Iwasaki, A., Gesch, D.B., Oimoen, M.J., Zhang, Z., Danielson, J.J., Krieger, T., Curtis, B., Haase, J., Abrams, M., Carabajal, C., 2011. ASTER global digital elevation model version 2 - summary of validation results.
- Thomas, C.D., Cameron, A., Green, R.E., Bakkenes, M., Beaumont, L.J., Collingham, Y.C., Erasmus, B.F.N., Siqueira, M.F. de, Grainger, A., Hannah, L., Hughes, L., Huntley, B., Jaarsveld, A.S. van, Midgley, G.F., Miles, L., Ortega-Huerta, M.A., Peterson, A.T., Phillips, O.L., Williams, S.E., 2004. Extinction risk from climate change. *Nature* 427, 5.
- Thompson, I.D., Mackey, B., McNulty, S., Mosseler, A., 2009. Forest resilience, biodiversity, and climate change: a synthesis of the biodiversity / resilience / stability relationship in forest ecosystems, CBD technical series. Secretariat of the Convention on Biological Diversity, Montreal.
- Urban, M.C., 2015. Accelerating extinction risk from climate change. *Science* 348, 571–573. <https://doi.org/10.1126/science.aaa4984>
- Walter, J.A., Stovall, A.E.L., Atkins, J.W., 2021. Vegetation structural complexity and biodiversity in the Great Smoky Mountains. *Ecosphere* 12, e03390. <https://doi.org/10.1002/ecs2.3390>
- White, Joanne.C., Wulder, M.A., Hobart, G.W., Luther, J.E., Hermosilla, T., Griffiths, P., Coops, N.C., Hall, R.J., Hostert, P., Dyk, A., Guindon, L., 2014. Pixel-based image compositing for large-area dense time series applications and science. *Canadian Journal of Remote Sensing* 40, 192212. <https://doi.org/10.1080/07038992.2014.945827>
- Zhu, Z., Woodcock, C.E., 2012. Object-based cloud and cloud shadow detection in Landsat imagery. *Remote Sensing of Environment* 118, 83–94. <https://doi.org/10.1016/j.rse.2011.10.028>